Chaos and weather prediction
January 2000

By **Roberto Buizza**[1]

European Centre for Medium-Range Weather

Abstract

The weather is a chaotic system. Small errors in the initial conditions of a forecast grow rapidly, and affect predictability. Furthermore, predictability is limited by model errors due to the approximate simulation of atmospheric processes of the state-of-the-art numerical models.

These two sources of uncertainties limit the skill of single, deterministic forecasts in an unpredictable way, with days of high/poor quality forecasts randomly followed by days of high/poor quality forecasts.

Two of the most recent advances in numerical weather prediction, the operational implementation of ensemble prediction systems and the development of objective procedures to target adaptive observations are discussed.

Ensemble prediction is a feasible method to integrate a single, deterministic forecast with an estimate of the probability distribution function of forecast states. In particular, ensemble can provide forecasters with an objective way to predict the skill of single deterministic forecasts, or, in other words, to forecast the forecast skill. The European Centre for Medium-Range Weather Forecasts (ECMWF) Ensemble Prediction System (EPS), based on the notion that initial condition uncertainties are the dominant source of forecast error, is described.

Adaptive observations targeted in sensitive regions can reduce the initial conditions' uncertainties, and thus decrease forecast errors. More generally, singular vectors that identify unstable regions of the atmospheric flow can be used to identify optimal ways to adapt the atmospheric observing system.

Table of contents

1. Corresponding author address: Dr Roberto Buizza, ECMWF, Shinfield Park, Reading RG2 9AX. Tel.:0118-9499653. Email: buizza@ecmwf.int

1. INTRODUCTION

A dynamical system shows a chaotic behavior if most orbits exhibit sensitive dependence (Lorenz 1993). An orbit is characterized by sensitive dependence if most other orbits that pass close to it at some point do not remain close to it as time advances.
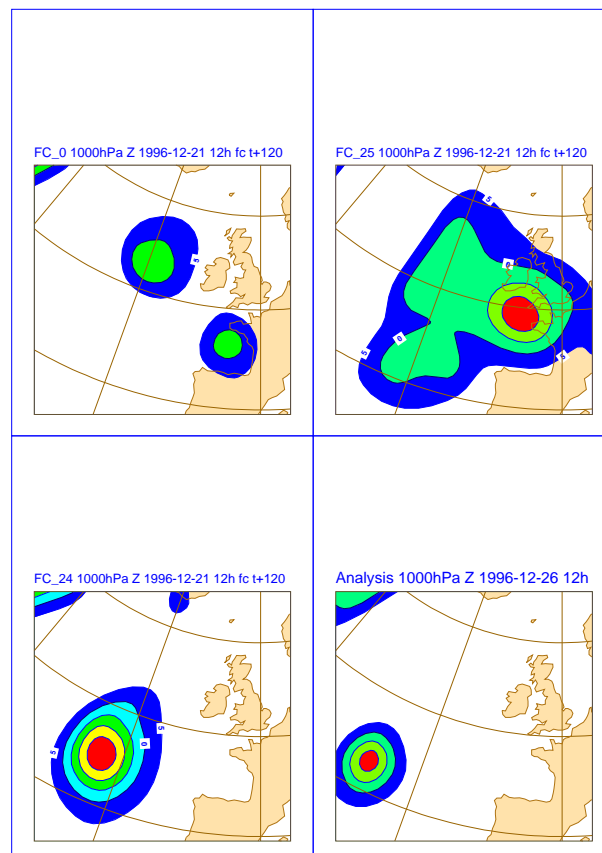

Figure 1. (a)-(c) Forecast for the geopotential height at 1000 hPa (this field illustrates the atmospheric state close to the surface) given by three forecasts started from very similar initial conditions, and (d) verifying analysis. Contour interval is 5 m, with only values smaller than 5 m shown.

The atmosphere exhibits this behavior. Fig. 1 shows three different weather forecasts, all started from very similar initial conditions. The differences among the three initial conditions were smaller than estimated analysis errors, and each of the three initial conditions could be considered as an equally probable estimate of the "true" initial state of the atmosphere. After 5 days of numerical integration, the three forecasts evolved into very different atmospheric situations. In particular, note the different positions of the cyclone forecast in the Eastern Atlantic approaching United Kingdom (Fig. 1 (a)-(c)). The first forecast indicated two areas of weak cyclonic circulation west and south of the British Isles; the second forecast positioned a more intense cyclone southwest of Cornwall, and the third forecast kept the cyclone in the open seas. This latter turned out to be the most accurate when compared to the observed atmospheric state (Fig. 1 (d). This is a typical example of orbits initially close together and then diverging during

time evolution.

The atmosphere is an intricate dynamical system with many degrees of freedom. The state of the atmosphere is described by the spatial distribution of wind, temperature, and other weather variables (e.g. specific humidity and surface pressure). The mathematical differential equations describing the system time evolution include Newton's laws of motion used in the form 'acceleration equals force divided by mass', and the laws of thermodynamics which describe the behavior of temperature and the other weather variables. Thus, generally speaking, there is a set of differential equations that describe the weather evolution, at least, in an approximate form.

Richardson (1922) can be considered the first to have shown that the weather could be predicted numerically. In his work, he approximated the differential equations governing the atmospheric motions with a set of algebraic difference equations for the tendencies of various field variables at a finite number of grid points in space. By extrapolating the computed tendencies ahead in time, he could predict the field variables in the future. Unfortunately, his results were very poor, both because of deficient initial data, and because of serious problems in his approach.

After World War II the interest in numerical weather prediction revived, partly because of an expansion of the meteorological observation network, but also because of the development of digital computers. Charney (1947, 1948) developed a model applying an essential filtering approximation of the Richardson's equations, based on the so-called geostrophic and hydrostatic equations. In 1950, an electronic computer (ENIAC) was installed at Princeton University, and Charney, Fjørtoft and Von Neumann & Ritchmeyer (1950) made the first numerical prediction using the equivalent barotropic version of Charney's model. This model provided forecasts of the geopotential height near 500 hPa, and could be used as an aid to provide explicit predictions of other variables as surface pressure and temperature distributions. Charney's results led to the developments of more complex models of the atmospheric circulation, the so-called global circulation models.

With the introduction of powerful computers in meteorology, the meteorological community invested more time and efforts to develop more complex numerical models of the atmosphere. One of the most complex models used routinely for operational weather prediction is the one implemented at the European Centre for Medium-Range Weather Forecasts (ECMWF). At the time of writing (December 1999), its is based on a horizontal spectral triangular truncation T319 with 60 vertical levels formulation (Simmons *et al*. 1989, Courtier *et al*. 1991, Simmons *et al*. 1995). It includes a parameterization of many physical processes such as surface and boundary layer processes (Viterbo & Beljaars 1995) radiation (Morcrette 1990), and moist processes (Tiedtke 1993, Jacob 1994).

The starting point, in mathematical terms the initial conditions, of any numerical integration is given by very complex assimilation procedures that estimate the state of the atmosphere by considering all available observations. The fact that a limited number of observations are available (limited compared to the degrees of freedom of the system) and that part of the globe is characterized by a very poor coverage introduces uncertainties in the initial conditions. The presence of uncertainties in the initial conditions is the first source of forecast errors.

A requirement for skilful predictions is that numerical models are able to accurately simulate the dominant atmospheric phenomena. The fact that the description of some physical processes has only a certain degree of accuracy, and the fact that numerical models simulate only processes with certain spatial and temporal, is the second source of forecast errors. Computer resources contribute to limit the complexity and the resolution of numerical models and assimilation, since, to be useful, numerical predictions must be produced in a reasonable amount of time.

These two sources of forecast errors cause weather forecasts to deteriorate with forecast time.

Initial conditions will always be known approximately, since each item of data is characterized by an error that depends on the instrumental accuracy. In other words, small uncertainties related to the characteristics of the atmospheric observing system will always characterize the initial conditions. As a consequence, even if the system equations were well known, two initial states only slightly differing would depart one from the other very rapidly

as time progresses (Lorenz 1965). Observational errors, usually in the smaller scales, amplify and through non-linear interactions spread to longer scales, eventually affecting the skill of these latter ones (Somerville 1979).

The error growth of the 10-day forecast of the ECMWF model from 1 December 1980 to 31 May 1994 was analyzed in great detail by Simmons *et al*. (1995). It was concluded that 15 years of research had improved substantially the accuracy over the first half of the forecast range (say up to forecast day 5), but that there had been little error reduction in the late forecast range. While this applied on average, it was also pointed out that there had been improvements in the skill of the good forecasts. In other words, good forecasts had higher skill in the nineties than before. The problem was that it was difficult to assess a-priori whether a forecast would be skilful or unskillful using only a deterministic approach to weather prediction.
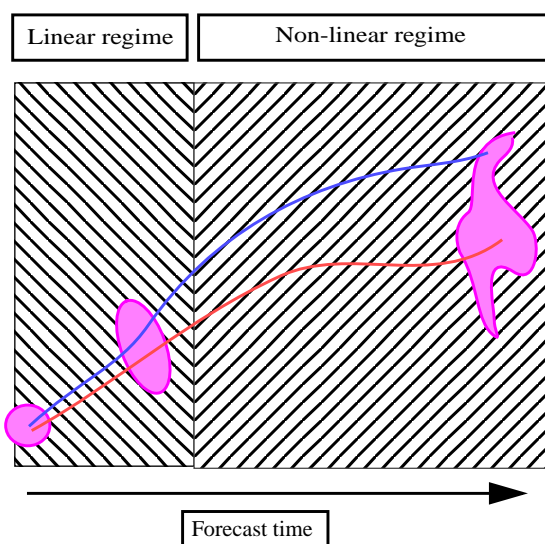

Figure 2. The deterministic approach to numerical weather prediction provides one single forecast (blue line) for the "true" time evolution of the system (red line). The ensemble approach to numerical weather prediction tries to estimate the probability density function of forecast states (magenta shapes). Ideally, the ensemble probability density function estimate includes the true state of the system as a possible solution.

Generally speaking, a complete description of the weather prediction problem can be stated in terms of the time evolution of an appropriate probability density function (PDF) in the atmosphere's phase space (Fig. 2). Although this problem can be formulated exactly through the continuity equation for probability (Liouville equation, see e.g. Ehrendorfer 1994), ensemble prediction based on a finite number of deterministic integrations appears to be the only feasible method to predict the PDF beyond the range of linear error growth. Ensemble prediction provided a way to overcome one of the problems highlighted by Simmons *et al*. (1995), since it can be used to estimate the forecast skill of a deterministic forecast, or, in other words, to forecast the forecast skill.

Since December 1992, both the US National Center for Environmental Predictions (NCEP, previously NMC) and ECMWF have integrated their deterministic high-resolution prediction with medium-range ensemble prediction (Tracton & Kalnay 1993, Palmer *et al*. 1993). These developments followed the theoretical and experimental work of, among others, Epstein (1969), Gleeson (1970), Fleming (1971a-b) and Leith (1974).

Both centres followed the same strategy of providing an ensemble of forecasts computed with the same model, one started with unperturbed initial conditions referred to as the "control" forecast and the others with initial conditions defined adding small perturbations to the control initial condition. Generally speaking, the two ensemble systems

differ in the ensemble size, in the fact that at NCEP a combination of lagged forecasts is used, and in the definition of the perturbed initial. The reader is referred to Toth & Kalnay (1993) for the description of the 'breeding' method applied at NMC and to Buizza & Palmer (1995) for a thorough discussion of the singular vector approach followed at ECMWF.

A different methodology was developed few years later at the Atmospheric Environment Service (Canada), where a system simulation approach was followed to generate an ensemble of initial perturbations (Houtekamer *et al*. 1996). A number of parallel data assimilation cycles is run randomly perturbing the observations, and using different parameterisation schemes for some physical processes in each run. The ensemble of initial states generated by the different data assimilation cycles defines the initial conditions of the Canadian ensemble system. Moreover, forecasts started from such an ensemble of initial conditions are used to estimate forecast-error statistics (Evensen 1994, Houtekamer & Mitchell 1998).

Ensemble prediction, which can be considered one of the most recent advances in numerical weather prediction, is the first topic discussed in this work. The development of objective procedures to target adaptive observations is the second topic on which attention will be focused.

The idea of targeting adaptive observations is based on the fact that weather forecasting can be improved by adding extra observations only in sensitive regions. These sensitive regions can be identified using tangent forward and adjoint versions of numerical weather prediction models (Thorpe *et al*. 1998, Buizza & Montani 1999). Once the sensitive regions have been localised, instruments can be sent to those locations to take the required observations using pilot-less aircraft, or energy-intensive satellite instruments can be switched on to sample them with greater accuracy.

After this Introduction, section 2 describes some early results by Lorenz, and illustrates the chaotic behavior of a simple 3-dimension system. In section 3 the main steps of numerical weather prediction are delineated. The impact of initial condition and model uncertainties on numerical integration is discussed in section 4. The ECMWF Ensemble Prediction System is described in section 5. Targeting adaptive observations using singular vectors is discussed in section 6. Some conclusions are reported in section 7. Some mathematical details are reported in two Appendices.

2. THE LORENZ SYSTEM

One of the fathers of chaos theory is Edward Lorenz (1963, 1965). Results from the 3-dimentional Lorenz system

$$
\begin{aligned}
\dot{X} &= -\sigma X + \sigma Y \\
\dot{Y} &= -XY + rX - Y \\
\dot{Z} &= XY - bZ
\end{aligned}
\tag{1}
$$

illustrate the dispersion of finite time integrations from an ensemble of initial conditions (Fig. 3). The different initial points can be considered as estimates of the "true" state of the system (which can be thought of as any point inside ellipsoid), and the time evolution of each of them as possible forecasts. Subject to the initial "true" state of the system, points close together at initial time diverge in time at different rates. Thus, depending on the point chosen to describe the system time evolution, different forecasts are obtained.

The two wings of the Lorenz attractor can be considered as identifying two different weather regimes, for example one warm and wet and the other cold and sunny. Suppose that the main purpose of the forecast is to predict whether the system is going through a regime transition. When the system is in a predictable initial state (Fig. 3 (a)), the

rate of forecast diverge is small, and all the points stay close together till the final time. Whatever the point chosen to represent the initial state of the system, the forecast is characterised by a small error, and a correct indication of a regime transition is given. The ensemble of points can be used to generate probabilistic forecasts of regime transitions. In this case, since all points end in the other wing of the attractor, there is a 100% probability of regime transition.

Figure 3. Lorenz attractor with superimposed finite-time ensemble integration.

By contrast, when the system is in a less predictable state (Fig. 3 (b)), the points stay close together only for a short time period, and then start diverging. While it is still possible to predict with a good degree of accuracy the future forecast state of the system for a short time period, it is difficult to predict whether the system will go through a regime transition in the long forecast range. Fig. 3 (c) shows an even worse scenario, with points diverging even after a short time period, and ending in very distant part of the system attractor. In probabilistic terms, one could have only predicted that there is a 50% chance of the system undergoing a regime transition. Moreover, the ensemble of points indicates that there is a greater uncertainty in predicting the region of the system attractor where the system will be at final time in the third case (Fig. 3 (c)).

The comparison of the points' divergence during the three cases indicates how ensemble prediction systems can be used to "forecast the forecast skill". In the case of the Lorenz system, a small divergence is associated to a predictable case, and confidence can be attached to any of the single deterministic forecasts given by the single points. By contrast, a large diverge indicate low predictability.
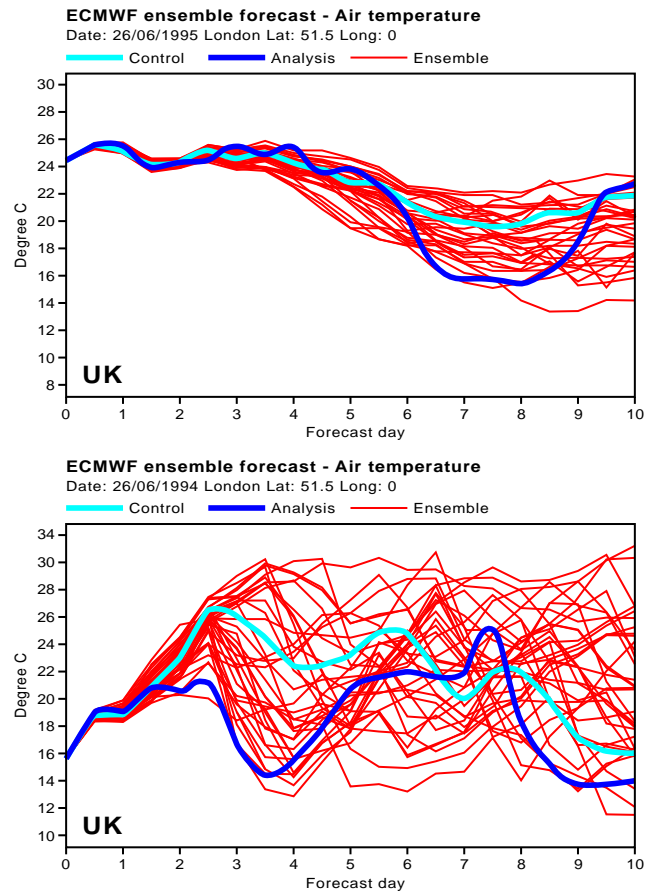
Figure 4. ECMWF forecasts for air temperature in London started from (a) 26 June 1995 and (b) 26 June 1994.

Similar sensitivity to the initial state is shown in weather prediction. Fig. 4 shows the forecasts for air temperature in London given by 33 different forecasts started from very similar initial conditions for two different dates, the 26th of June of 1995 and the 26th of June 1994. There is a clear different degree of divergence during the two cases. All forecasts stay close together up to forecast day 10 for the first case (Fig. 4 (a)), while they all diverge already at forecast day 3 in the second case (Fig. 4 (b)). The level of spread among the different forecasts can be used as a measure of the predictability of the two atmospheric states.

3. NUMERICAL WEATHER PREDICTION

Numerical weather prediction is realised by integrating primitive-equation models. The equations are solved by replacing time-derivatives by finite differences, and spatially either by finite difference schemes or spectral methods. The state of the atmosphere is described at a series of grid-points by a set of state variables such as temperature, velocity, humidity and pressure.

At the time of writing (December 1999) the ECMWF high-resolution deterministic model has a spectral triangular truncation TL319, which is equivalent to a grid-point spacing of about 60 km at mid-latitudes (Fig. 5) and 60 vertical levels (Fig. 6).
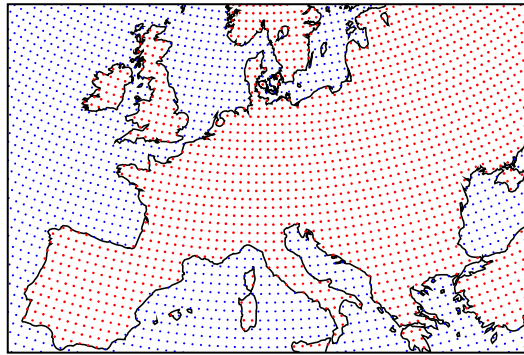
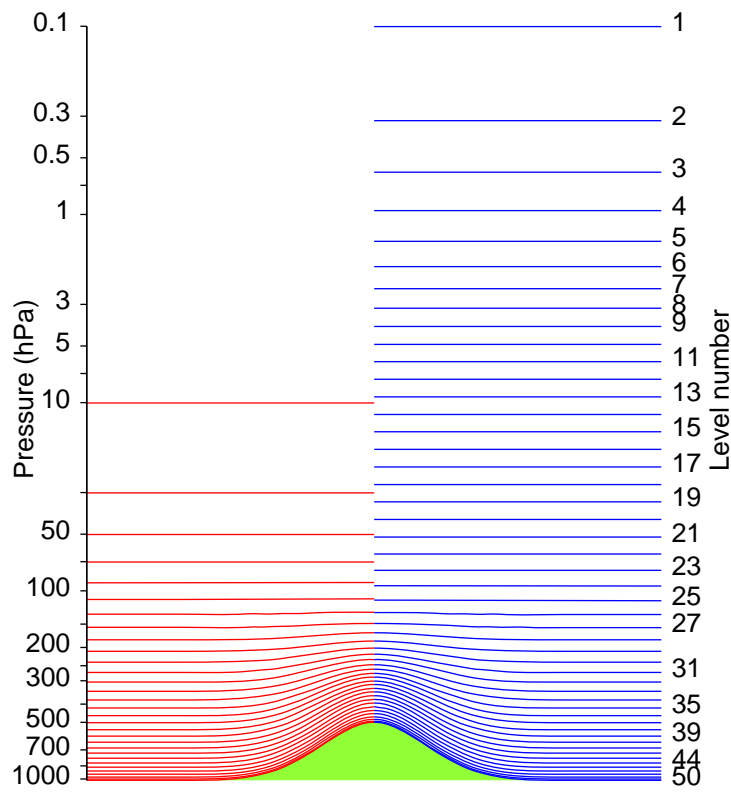Figure 5. Grid-points over Europe of the ECMWF model.

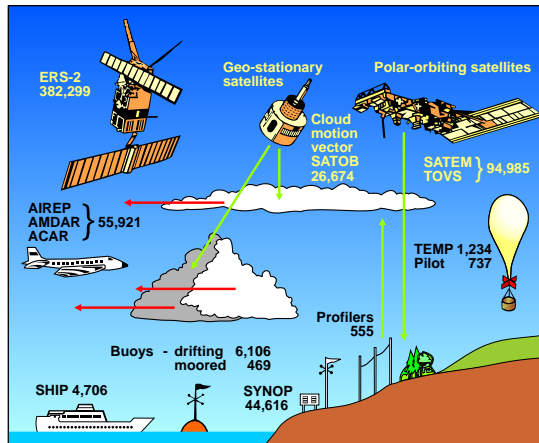Figure 6. Vertical levels of the ECMWF model.

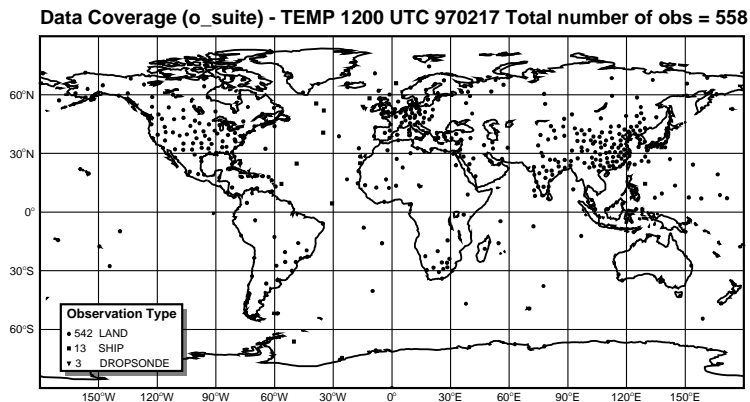Figure 7. Type and number of observations used to estimate the atmosphere initial conditions in a typical day.

Figure 8. Map of radiosonde locations.

Meteorological observations made all over the world (Fig. 7) are used to compute the best estimate of the system initial conditions. Some of these observations, such as the ones from weather balloons or radiosondes, are taken at specific times at fixed locations (Fig. 8). Other data, such as the ones from aircrafts, ships or satellites, are not fixed in space. Generally speaking, there is a great variability in the density of the observation network. Data over oceanic regions, in particular, are characterised by very coarse resolution.

Observations cannot be used directly to start model integration, but must be modified in a dynamically consistent way to obtain a suitable data set. This process is usually referred to as data assimilation. At the time of writing (December 1999), ECMWF uses a 4-dimensional data assimilation scheme to estimate the actual state of the atmosphere (Courtier *et al.* 1994).

In the ECMWF model, dynamical quantities as pressure and velocity gradients are evaluated in spectral space, while computations involving processes such as radiation, moisture conversion, turbulence, are calculated in gridpoint space. This combination preserves the local nature of physical processes, and retains the superior accuracy of the spectral method for dynamical computation.

The physical processes associated with radiative transfer, turbulent mixing, moist processes, are active at scales smaller than the horizontal grid size. The approximation of unresolved processes in terms of model-resolved variables is referred to as parameterisation (Fig. 9). The parameterisation of physical processes is probably one of the

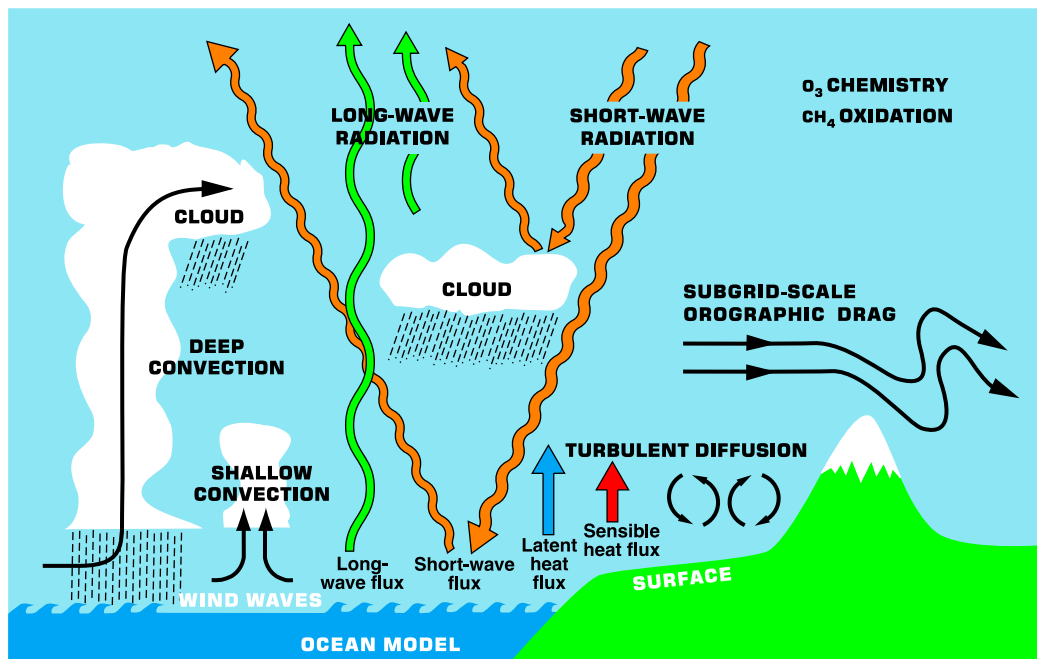most difficult and controversial area of weather modelling (Holton 1992).

Figure 9. Schematic diagram of the different physical processes represented in the ECMWF model.

4. SOURCES OF FORECAST ERROR

It has been already mentioned that uncertainties in the initial conditions and in the model are both sources of forecast error. Some indications of the relative importance of the two sources can be deduced from the works of Downton & Bell (1988) and Richardson (1998), who compared forecasts given by the UKMO (United Kingdom Meteorological Office) and the ECMWF forecasting systems. In these studies, substantial forecast differences between the ECMWF and the UKMO operational forecasts could mostly be traced to differences between the two operational analyses, rather than between the two forecast models. On the other hand, recent results from Harrison *et al*. (1999) indicate that the impact of model uncertainties on forecast error cannot be ignored.

These results suggest that an ensemble system should certainly simulate the presence of uncertainties in the initial conditions, since this is the dominant effect, but it should also simulate model uncertainties.

The first version of the ECMWF Ensemble Prediction System (hereafter EPS, Palmer *et al*. 1993, Molteni *et al*. 1996) implemented operationally in December 1992 included only a simulation of initial uncertainties. A similar "perfect model" strategy was followed at the US National Centers for Environmental Prediction (NCEP, Tracton & Kalnay 1993).

Houtekamer *et al*. (1996) first included model uncertainties in the ensemble prediction system developed at the Atmospheric Environment Service in Canada. Following a system simulation approach to ensemble prediction, they developed a procedure where each ensemble member differs both in the initial conditions, and in sub-grid scale parameters. In this approach, each ensemble member is integrated using different parameterizations of horizontal diffusion, convection, radiation, gravity wave drag, and with different orography.

There are certainly good grounds for believing that there is a significant source of random error associated with the parameterized physical processes. For example, consider a grid point over the tropical warm pool area during a

period of organized deep convection. By definition, the actual contributions to the tendencies due to parameterized physical processes are often associated with organized mesoscale convective systems whose spatial extent may be comparable with the model resolution. In such a case, the notion of a quasi-equilibrium ensemble of sub-grid-scale processes, upon which all current parameterizations schemes are based, cannot be a fully-appropriate concept for representing the actual parameterized heating (Palmer 1997). For example, even if the parameterized heating fields agree on average (i.e. over many time steps) at the chosen grid point, there must inevitably be some standard deviation in the time-step by time-step difference between observed and modeled heating.

Since October 1998, a simple stochastic scheme for simulating random model errors due to parameterized physical processes has been used in the ECMWF EPS (Buizza *et al*. 1999). The scheme is based on the notion that the sort of random error in parameterized forcing are coherent between the different parameterization modules, and have certain coherence on the space and time scales associated, for example, with organized convection schemes. Moreover, the scheme assumes that the larger the parameterized tendencies, the larger the random error component will be. The notion of coherence between modules allows the stochastic perturbation to be based on the total tendency from all parameterized processes, rather than on the parameterized tendencies from each of the individual modules. In this respect the ECMWF scheme differs conceptually from that of Houtekamer *et al*. (1996). More details about the scheme are reported in the following section.

5. THE ECMWF ENSEMBLE PREDICTION SYSTEM

Routine real-time execution of the ECMWF EPS started in December 1992 with a 31-member T63L19 configuration (spectral triangular truncation T63 and 19 vertical levels, Palmer *et al*. 1993, Molteni *et al*. 1996). A major upgrade to a 51-member TL159L31 system (spectral triangular truncation T159 with linear grid) took place in 1996 (Buizza *et al*. 1998). A scheme to simulate model uncertainties due to random model error in the parameterized physical processes was introduced in 1998.

5.1 The original EPS configuration

Schematically, each ensemble member e_j was defined by the time integration

$$e_j(t) = \int_{t=0}^{t} [A(e_j, t) + P(e_j, t)] \, \mathrm{d}t \tag{2}$$

of the model equations

$$\frac{\partial e_j}{\partial t} = A(e_j, t) + P(e_j, t) \tag{3}$$

starting from perturbed initial conditions

$$e_j(t = 0) = e_0(t = 0) + \delta e_j(t = 0) \tag{4}$$

where A and P identify the contribution to the full equation tendency of the non-parameterized and parameterized physical processes, and where $e_0(t = 0)$ is the operational analysis at $t = 0$.

The initial perturbations $\delta e_j(t = 0)$ were generated using the singular vectors of the linear version of the ECMWF, computed to maximize the total energy norm over a 48-hour time interval (Buizza & Palmer 1995), and scaled to have an amplitude comparable to analysis error estimates.

The singular vectors of the tangent forward propagator sample the phase space directions of maximum growth during a 48-hour time interval. Small errors in the initial conditions along these directions would amplify most rapidly, and affect the forecast accuracy. The reader is referred to Appendix A for a more complete mathematical definition of the singular vectors.

Fig. 10 illustrates the typical structure of the leading singular vector used to generate the ensemble of initial perturbations for 17 January 1997. Total energy singular vectors are usually located in the lower troposphere at initial time, with total energy peaking at between around 700 hPa (i.e. around 3000 m), in regions of strong barotropic and baroclinic energy conversion (Buizza & Palmer 1995). During their growth, they show an upscale energy transfer and upward energy propagation. Results have indicated a very good agreement between the regions where singular vectors are located and other measures of baroclinic instability such as the Eady index introduced by Hoskins & Valdes (1990). This is shown in Fig. 11 for the case of 17 January 1997. The reader is referred to Hoskins *et al.* (1999) for recent investigations on singular vector growth mechanisms.
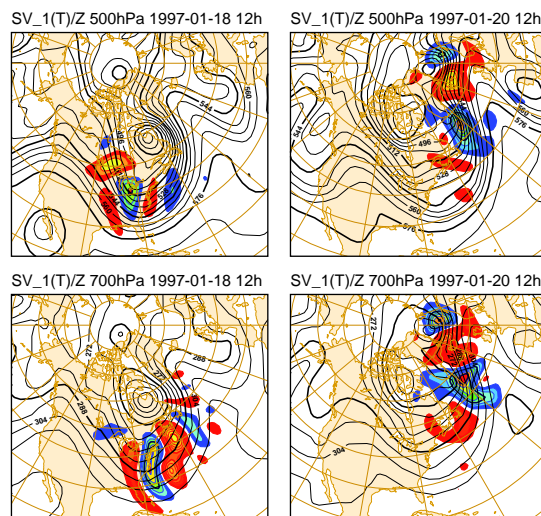

Figure 10. Most unstable singular vector growing between 17 and 19 January 1997 at initial (left panels) and final (right panels) times. The top panels show the singular vector temperature component (shaded blue/green for negative and shaded yellow/red for positive values) and the atmospheric state (geopotential height) at 500 hPa (i.e. approximately at 5000 m). Bottom panels are as top panels but for 700 hPa (i.e. approximately at 3000 m). Contour interval is 8 dam for geopotential height, and 0.2 degrees for temperature at initial time and 1.0 degree at final time.

Eady index 1997-01-18/20
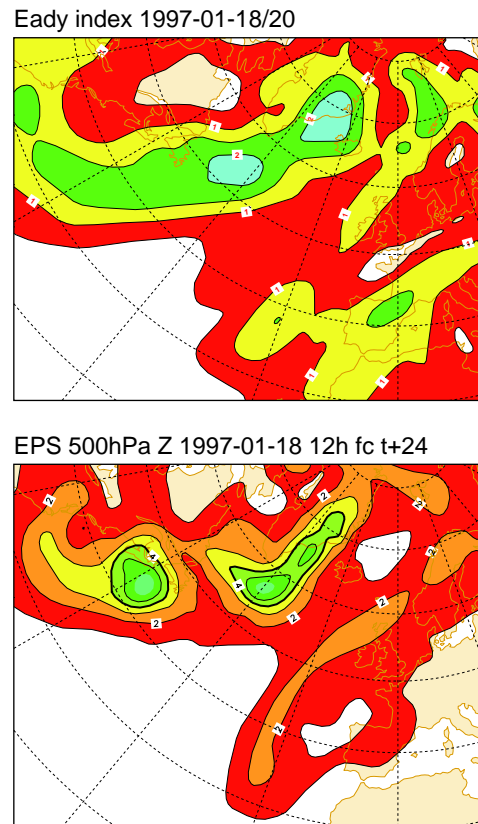
EPS 500hPa Z 1997-01-18 12h fc t+24

Figure 11. Eady index (top panel) and location of the leading singular vectors identified by the root-mean-square amplitude of the EPS perturbations at forecast day 1 (bottom panel) for the case of 17 January 1997. Contour interval is 1 day-1 for the Eady index, and 1 m for the EPS perturbation amplitude.

Until 26 March 1998, the EPS initial perturbations were computed to sample instabilities growing in the forecast range, and no account was taken of perturbations that had grown during the data assimilation cycle leading up to the generation of the initial conditions (Molteni *et al*. 1996).

A way to overcome this problem is to use singular vectors growing in the past, and evolved to the current time.

The 50 perturbed initial conditions were generated by adding and subtracting 25 perturbations defined using 25 singular vectors selected from computed singular vectors so that they do not overlap in space. The selection criteria were that the leading 4 singular vectors are always selected, and that subsequent singular vectors are selected only if less than 50% of their total energy cover a geographical region where already 4 singular vectors are located.

Once the 25 singular vectors were selected, an orthogonal rotation in phase-space and a final re-scaling were performed to construct the ensemble perturbations. The purpose of the phase-space rotation is to generate perturbations with the same globally averaged energy as the singular vectors, but smaller local maxima and a more uniform spatial distribution. Moreover, unlike the singular vectors, the rotated singular vectors are characterized by similar amplification rates (at least up to 48 hours). Thus, the rotated singular vectors diverge, on average, equally from the control forecast. The rotation is defined to minimize the local ratio between the perturbation amplitude and the amplitude of the analysis error estimate given by the ECMWF data assimilation procedure. The re-scaling allowed perturbations to have local maxima up to $\alpha = \sqrt{0.6}$ larger than the local maxima of the analysis error estimate.

A way to take into account perturbations growing during the data assimilation period was to generate the EPS initial perturbation using two sets of singular vectors. In mathematical terms, since 26 March 1998 (Barkmeijer *et al*.

1999a) the day d initial perturbations have been generated using both the singular vectors growing in the forecast range between day d and day $d + 2$ at initial time, and the singular vectors that had grown in the past between day $d - 2$ and day d at final time

$$\delta e_j(t = 0) \ = \ \sum_{i = 1}^{25} [\alpha_{i,j} v_i^{d, d + 2}(t = 0) + \beta_{i,j} v_i^{d - 2, d}(t = 48 \text{ h})] \tag{5}$$

where $v_i^{d, d + 2}(t = 0)$ is the i-th singular vector growing between day d and d+2 at time t=0. The coefficients ai,j and bi,j set the initial amplitude of the ensemble perturbations, and are defined by comparing the singular vectors with estimates of analysis errors (Molteni *et al.* 1996). Since 26 March 1998, the selection criteria has been kept as before, but a new scaling factor $\alpha \ = \ \sqrt{0.5}$ has been used.

The initial perturbations are specified in terms of the spectral coefficients of the 3-dimensional vorticity, divergence and temperature fields (no perturbations are defined for the specific humidity since the singular vector computation is performed with a dry linear forward/adjoint model), and of the 2-dimensional surface pressure field. They are added and subtracted to the control initial conditions to define perturbed initial conditions. Then, 50 + 1 (control) 10-day T_L159L31 non-linear integrations are performed.

With the current ECMWF computer facilities, each day the whole EPS (10-day integration, 51 members at T_L159L40 with T42L40 singular vectors computed for the Northern and the Southern Hemispheres) takes approximately 150 hours of total computing time (about 10% of this time is used to compute the initial perturbations). By contrast, the high resolution T_L319L60 deterministic forecast (10-day integration) takes about 40 hours, and the data assimilation procedure used to generate the unperturbed initial conditions takes about 120 hours (4 cycles per day, once every 6 hours).

5.2 The new EPS configuration

In October 1998, a scheme to simulate random model errors due to parameterized physical processed was introduced (Buizza *et al.* 1999). This scheme can be considered as a simple first attempt to simulated random model errors due to parametrized physical processes. It is based on the notion that random errors due to parametrized physical processes are coherent between the different parametrization modules and have a certain coherence on the space and time scales represented by the model. The scheme assumes that the larger the parametrized tendencies, the larger the random error component.

In the new EPS, each ensemble member e_j can be seen as the time integration

$$e_j(t) \ = \ \int_{t = 0}^{t} [A(e_j, t) + P_j{}'(e_j, t)] \, dt \tag{6}$$

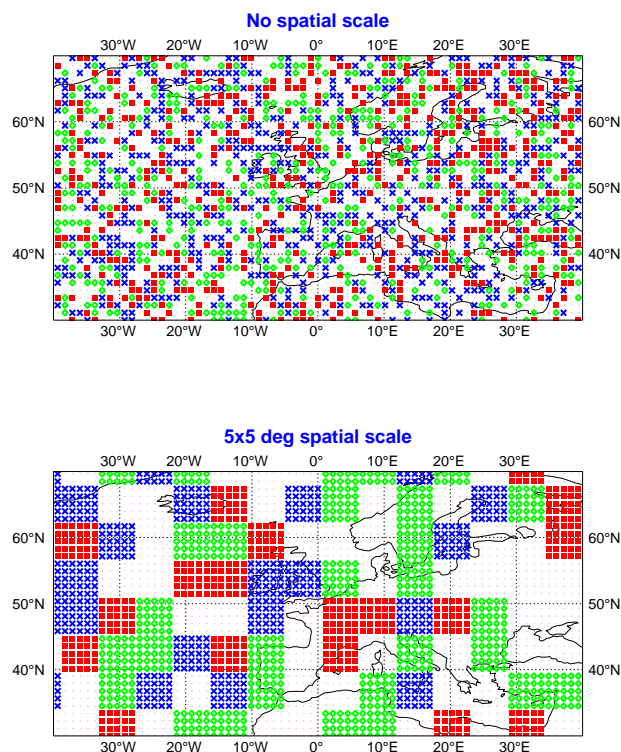of the perturbed model equations

$$\frac{\partial e_j}{\partial t} \ = \ A(e_j, t) + P_j{}'(e_j, t) \tag{7}$$

starting from the perturbed initial conditions defined in Eq. (1), where A and P' identify the contribution to the full equation tendency of the non-parameterized and parameterized physical processes. For each grid point $x = (\lambda, \phi, \sigma)$ (identified by its latitude, longitude and vertical hybrid coordinate), the perturbed parameterized tendency (of each state vector component) is defined as

$$P_j{'}(e_j, t) = [1 + \langle r_j(\lambda, \phi, \sigma) \rangle_{D,T}]P(e_j, t) \tag{8}$$

where P is the unperturbed diabatic tendency, and $\langle ... \rangle_{D,T}$ indicates that the same random number r_j has been used for all grid points inside a $D \times D$ degree box and over T time steps.

The notion of space-time coherence assumes that organized systems have some intrinsic space and time-scales that may span more than one model time step and more than one model grid point. Making the stochastic uncertainty proportional to the tendency is based on the concept that organization (away from the notion of a quasi-equilibrium ensemble of sub-grid processes) is likely to be stronger, the stronger is the parameterized contribution. A certain space-time correlation is introduced in order to have tendency perturbations with the same spatial and time scales as observed organization.

Figure 12. Random numbers used to perturb the tendencies due to parameterised physical processes. The top panel shows the case of no spatial scale, in other words when different random numbers are used at each grid-point. The bottom panel shows the case when the same random number was used for grid-points inside 5-degree boxes. Blue crosses identify grid-points with random numbers $-0.5 \leq \eta \leq -0.3$, green diamonds points with $-0.1 \leq \eta \leq 0.1$, and red squares points with $0.3 \leq \eta \leq 0.5$.

Fig. 12 shows a map of the random numbers used in a configuration tested when developing the so-called stochastic physics scheme. Fig. 12 (a) shows the matrix of random numbers r_j when each grid-point was assigned an independent value, while Fig. 12 (b) shows the matrix when the same random number was used inside 5 degree boxes. Results indicated that even perturbations without any spatial structure (i.e. with random numbers as in Fig.

12 (a)) had a major impact on 10-day model integrations (Buizza *et al*. 1999).

After an extensive experimentation, it was decided to implement in the operational EPS the stochastic physics scheme with random numbers sampled uniformly in the interval $[-0.5, 0.5]$, a 10 degrees box size ($D = 10$), and a 6 hours time interval ($T = 6$).

6. TARGETED OBSERVATIONS

Consider a meteorological system evolving between time t_0 and t, localised at final time t inside a geographical area Σ_t (hereafter verification area). Suppose that extra observations could be taken inside a geographical area Σ_0 at initial time t_0 (hereafter target area), with the purpose of improving the time t forecast inside Σ.

Singular vectors with maximum energy at final time inside a verification area can be used to identify the target area where extra observation should be taken, at initial time, to reduce the forecast error inside the verification area itself (Buizza & Montani 1999). The reader is referred to Appendices A and B for a more complete description of the mathematical formulation.

Other strategies can be used to target adaptive observations. Langland & Rohaly (1996), following the work of Rabier *et al*. (1996) on sensitivity vectors, proposed to use the lower tropospheric vorticity of the forecast state as cost function, and to target the region where the sensitivity field is maximum. A similar technique, but based on the use of a quasi-inverse linear model, was proposed by Pu *et al*. (1997, 1998). Bishop & Toth (1998) introduced the Ensemble Transform technique, in which linear combinations of ensemble perturbations are used to estimate the prediction error variance associated with different possible deployments of observational resources. Finally, following Hoskins *et al*. (1985) and Appenzeller *et al*. (1996), a more subjective strategy based on the use of potential vorticity to analyse atmospheric was also developed.

All these techniques were applied to target observations for the first time during FASTEX, the Fronts and Atlantic Storm Track Experiment (Joly *et al*. 1996, Thorpe & Shapiro 1995, Snyder 1996).

The focus of the FASTEX campaign was the extra-tropical cylonic storms that form over the western and mid Atlantic Ocean, and take about 2 days to develop and move towards Europe. Forecast failures are often associated with these very active atmospheric phenomena.

Fig. 13 shows the tracks of one of the storms observed during FASTEX, IOP 17 (IOP stands for Intensive Observation Period), and the location of various aircrafts that made additional observations between 17 and 19 February 1997 (Montani *et al*. 1999). Singular vectors, computed to have maximum total energy inside a verification region centred on the British Isles, were used to identify the most sensitive regions where observations were made. The comparison of the central pressure of two forecasts, one started from initial conditions computed with and one without the extra observations, with the observed value (Fig. 14) indicates that additional, targeted observations can improve the forecast accuracy. Fig. 15 shows the average impact of the targeted observations on the forecast error. Results indicated up to 20% forecast error reduction.

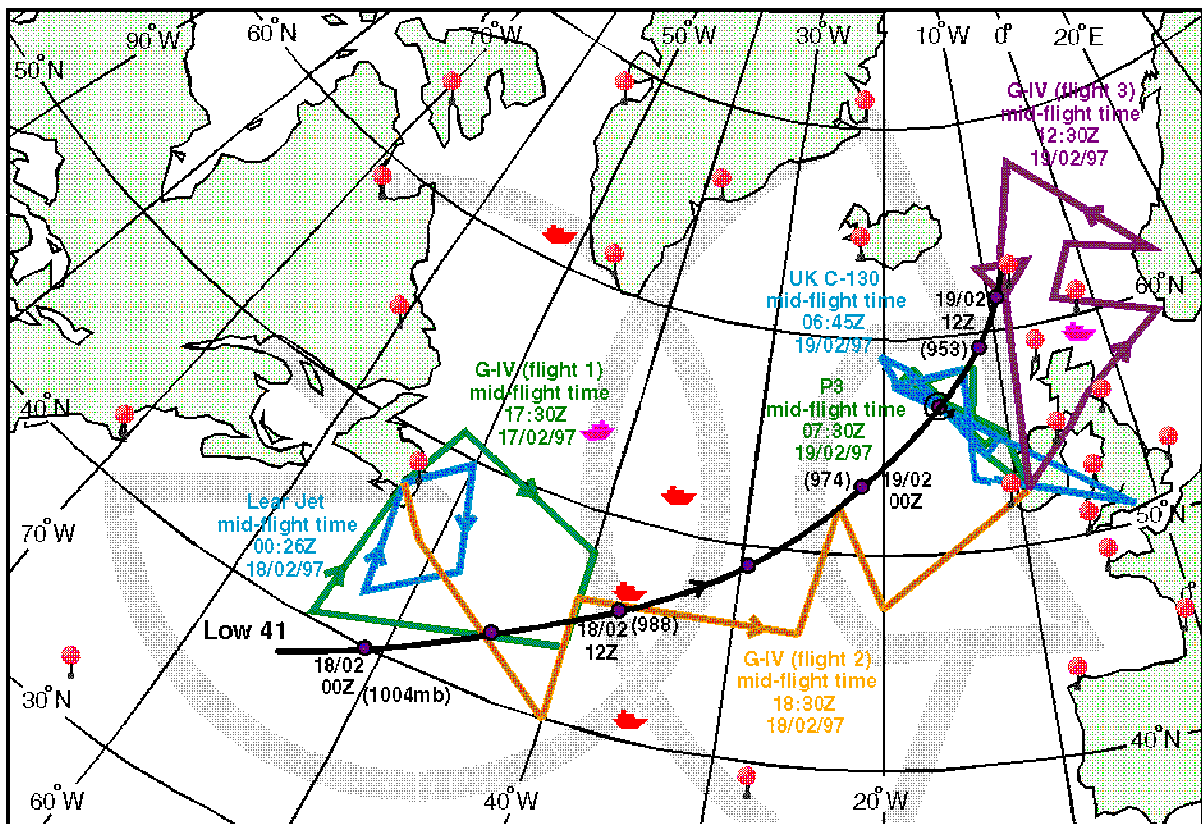FASTEX IOP17 Low 41 15Z 17/02/97 - 15Z 19/02/97

Figure 13. Map summarising the extra observations taken during the FASTEX experiment for IOP 17. The black track identifies the location of the cyclone minimum pressure, the coloured tracks the aircraft missions, and the red symbols additional radio-soundings (from Montani *et al.* 1999).
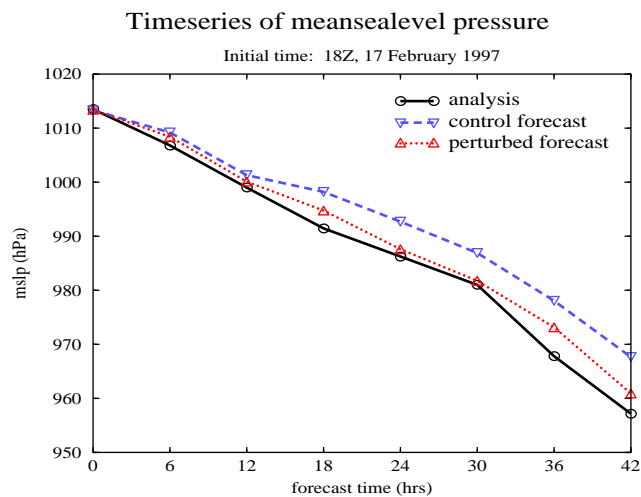

Figure 14. 6-hourly time series of the cyclone central pressure forecast without (blue dash line) and with (red dotted line) extra observations, and observed (black solid line), for IOP 17 (from Montani *et al.* 1999).
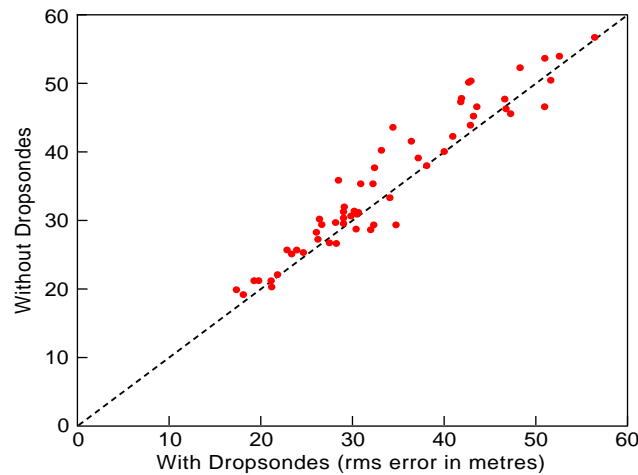
Figure 15. Scatter plot of the mean forecast errors with (x-axis) and without (y-axis) the extra observations, for the 500 and 1000 hPa geopotential height fields over Europe and North Atlantic at forecast day 2, 2.5 and 3 (from Montani *et al*. 1999).

Following the FASTEX campaign, other experiments were performed (e.g. NORPEX, the North Pacific Experiment, CALJET, the California Land-falling Jets experiments). All results confirmed that taking extra observations in sensitive regions could reduce forecast errors.

Robotic aerosondes capable of long-range monitoring could be used operationally in a very near future to fill chronic gaps in the global upper-air sounding network (Holland *et al*. 1992), and take extra observations in objectively identified regions. This follows years of intensive research at the Bureau of Meteorology of Melbourne, Australia, that culminated with the first-ever unmanned aircraft crossing of the Atlantic Ocean in August 1998 (http://www.aerosonde.com/opshist.htm).

7. SUMMARY AND FUTURE DEVELOPMENTS

Two of the most important advances in numerical weather prediction of the last 10 years, the operational implementation of ensemble prediction systems and the development of objective techniques to target adaptive observations, have been discussed.

Ensemble systems provide a possible way to estimate the probability distribution function of forecast states. They have been developed following the notion that uncertainties in the initial conditions and in the model formulation are the main sources of forecast errors. Results have demonstrated that a probabilistic approach to weather prediction can provide more information than a deterministic approach based on a single, deterministic forecast.

Ensemble prediction systems are particularly useful, if not necessary, to provide early warnings of extreme weather events. For example, ensemble systems can be used to predict probabilities of intense precipitation events (Fig. 16). Global ensemble systems can be used to provide boundary and initial conditions for higher-resolution, limited area ensemble prediction systems (Molteni *et al*. 1999, Marsigli *et al*. 1999).
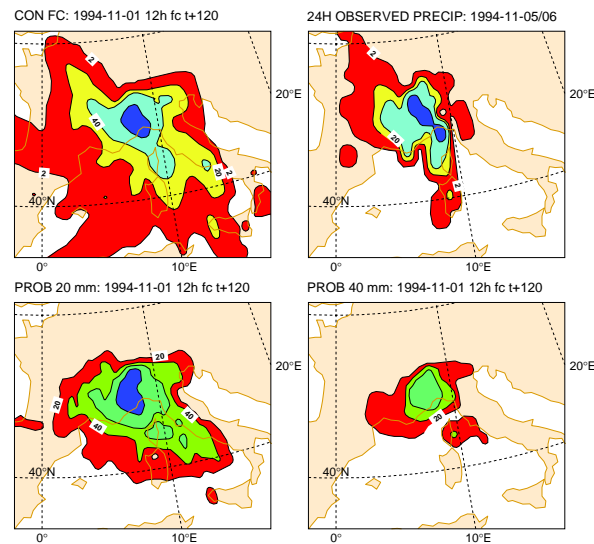
Figure 16. High-resolution TL319L31 forecasts for the flood in Piemonte, Italy, 5-6 November 1994. (a) Precipitation forecast, accumulated between t+96 h and t+120 h, predicted by the control forecast. (b) Observed precipitation field. (c) Ensemble probability forecast of more than 20 mm/d of precipitation. (d) Ensemble probability forecast of more than 40 mm/d of precipitation. Contour isolines 2, 20, 40 and 100 mm/d for precipitation, and every 20% for probabilities.

At ECMWF, work is in progress in many different areas to further improve the current ensemble prediction system.

Linearized versions of the most important physical processes have been developed (Mahfouf 1999), and investigation into the behaviour of the linear models in the computation of tropical singular vectors has started. The tropical target area has been chosen because the current EPS lacks perturbations of the initial condition in this area, where moist processes are of key importance. Results (Barkmeijer *et al*. 1999b, Puri *et al*. 1999) indicate that the inclusion of tropical singular vectors is essential in cases of hurricane prediction. Results indicate that tropical singular vectors are needed to generate a realistic spread among the ensemble of hurricane tracks.

The operational initial perturbations of the ECMWF EPS are constructed using singular vectors with maximum total energy growth. Total energy singular vectors have no knowledge of analysis error statistics. Generally speaking, it would be desirable to use information about analysis error characteristics in the singular vector computation. One way of improving upon this is to use in the singular vector computation statistics generated by the data assimilation system. Work is in progress to use the Hessian of the cost function of the 3-dimensional (or 4-dimensional) variational assimilation system (3D/4D-Var) to define singular vectors (Barkmeijer *et al*. 1998). These so-called Hessian singular vectors are constrained at initial time by analysis error statistics but still produce fast perturbation growth during the first few days of the forecast.

Work is in progress to investigate whether a so-called consensus analysis, defined as the average of analyses produced by different weather centres, is a better estimate of the atmospheric initial state than the ECMWF analysis (Richardson, 1999, personal communication). The operational EPS configuration has been run from the consensus analysis, average of the ECMWF, UKMO (UK Meteorological Office), Météo-France, NCEP (National Centers for Environmental Prediction, Washington) and DWD (Deutscher WetterDienst, Offenbach) analyses. The same perturbations as used in the operational EPS have been added to the consensus analysis to create the 50 perturbed initial conditions. Preliminary results show that the skill of the control forecast is improved if the consensus analysis is used instead of the ECMWF analysis as the unperturbed initial condition. Results also indicate that the difference between the spread in the two systems is rather small, while the ensemble-mean forecast of the system

started from the consensus analysis is more skilful.

Experimentation has started to verify whether a resolution increase from Tl159 to Tl255, and from 31 to 60 vertical levels would improve the EPS performance. Preliminary studies of the impact of an increase in horizontal resolution indicate that precipitation prediction improves substantially as resolution increases.

Finally, an ensemble approach to data assimilation is under test. Following Houtekamer *et al.* (1996), but with the ECMWF approach to represent model uncertainties, work has started at ECMWF to generate an ensemble of initial perturbations using the ECMWF 3D/4D-Var data assimilation. The purpose of this work is to investigate whether a better estimate of the "true" state of the atmosphere can be computed using this probabilistic approach.

8. CONCLUSION

The weather is a chaotic system, and numerical weather prediction is a very difficult task.

This work has demonstrated that the application of linear algebra (i.e. the use of singular vectors computed by solving an eigenvalue problem defined by the tangent forward and adjoint versions of the model) to meteorology can help in designing new ways to numerical weather prediction (Buizza 1997).

The same technique can be applied to any dynamical system, in particular to very complex systems with a large dimension. The basic idea is that there are only few, important directions of the phase-space of any system along which the most important processes occur. A successful prediction of the system time evolution should sample these directions, and describe the system evolution along them.

9. ACKNOWLEDGEMENTS

The ECMWF Ensemble Prediction System is the result of the work of many ECMWF staff members and consultants. It is based on the Integrated Forecasting System/Arpege software, developed in collaboration by ECMWF and Meteo-France. The work of many ECMWF and Meteo-France staff and consultants is acknowledged. I am grateful to Robert Hine for all his editorial help.

APPENDIX A SINGULAR VECTOR DEFINITION

Farrell (1982), studying the growth of perturbations in baroclinic flows, showed that, although the long time asymptotic behavior is dominated by discrete exponentially growing normal modes when they exist, physically realistic perturbations could present, for some finite time intervals, amplification rates greater than the most unstable normal mode amplification rate. Subsequently, Farrell (1988, 1989) showed that perturbations with the fastest growth over a finite time interval could be identified solving the eigenvalue problem of the product of the tangent forward and adjoint model propagators. His results supported earlier conclusions by Lorenz (1965) that perturbation growth in realistic models is related to the eigenvalues of the operator product.

Kontarev (1980) and Hall and Cacuci (1983) first used the adjoint of a dynamical model for sensitivity studies. Later on, Le Dimet & Talagrand (1986) proposed an algorithm, based on an appropriate use of an adjoint dynamical equation, for solving constraint minimization problems in the context of analysis and assimilation of meteorological observations. More recently, Lacarra & Talagrand (1988) applied the adjoint technique to determine optimal perturbations using a simple numerical model. Following Urban (1985) they used a Lanczos algorithm (Strang, 1986) in order to solve the related eigenvalue problem. For a bibliography in chronological order of published works in meteorology dealing with adjoints up to the end of 1992, the reader is referred to Courtier *et al.* (1993).

After Farrell and Lorenz, calculations of perturbations growing over finite-time intervals were performed, for example, by Borges & Hartmann (1992) using a barotropic model, and by Molteni & Palmer (1993) using a barotropic and a 3-level quasi-geostrophic model at spectral triangular truncation T21. Buizza (1992) and Buizza *et al*. (1993) first identified singular vectors in a primitive equation model with a large number of degrees of freedom.

Let χ be the state vector of a generic autonomous system, whose evolution equations can be formally written as

$$\frac{\partial \chi}{\partial t} = A(\chi) \tag{9}$$

Denote by $\chi(t)$ an integration of Eq. (9) from t_0 to t, which generates a trajectory from an initial point χ_0 to $\chi_1 = \chi(t)$. The time evolution of a small perturbation x around the time evolving trajectory $\chi(t)$ can be descibed, in a first approximation, by the linearized model equations

$$\frac{\partial x}{\partial t} = A_l x \tag{10}$$

where $A_l = \left.\frac{\partial A(x)}{\partial x}\right|_{\chi(t)}$ is the tangent operator computed at the trajectory point $\chi(t)$.

Let $L(t, t_0)$ be the integral forward propagator of the dynamical equations linearized about a non-linear trajectory $\chi(t)$

$$x(t) = L(t, t_0)x(t_0) \tag{11}$$

that maps a perturbation x at initial time t_0 to the optimization time t. The tangent forward operator L maps the tangent space Π_0, the linear vector space of perturbations at χ_0, to Π_1, the linear vector space at χ_1.

Consider two perturbations x and y, e.g. at χ_0, a positive definite Hermitian matrix E, and define the inner product $(...;...)_E$ as

$$(x;y)_E = \langle x;Ey \rangle \tag{12}$$

on the tangent space Π_0 in this case, where $\langle ...;... \rangle$ identifies the canonical Euclidean scalar product,

$$\langle x;y \rangle = \sum_{i=1}^{N} x_i y_i \tag{13}$$

Let $\|...\|_E^2$ be the norm associated with the inner product $(...;...)_E$

$$\|x\|_E^2 = (x;x)_E = \langle x;xE \rangle \tag{14}$$

Let L^{*E} be the adjoint of L with respect to the inner product $(...;...)_E$,

$$(L^{*E}x;y)_E = (x;Ly)_E \tag{15}$$

The adjoint of L with respect to the inner product defined by E can be written in terms of the adjoint L^* defined with respect to the canonical Euclidean scalar product,

$$L^{*E} = E^{-1}L^*E \tag{16}$$

From Eqs. (11) and (16) it follows that the squared norm of a perturbation x at time t is given by

$$\|x(t)\|_E^2 = (x(t_0);L^{*E}Lx(t_0))_E \tag{17}$$

Equation (17) shows that the problem of finding the phase space directions x for which $\|x(t)\|_E^2 / \|x(t_0)\|_E^2$ is maximum can be reduced to the search of the eigenvectors $v_i(t_0)$

$$L^{*E}Lv_i(t_0) = \sigma_i^2 v_i(t_0) \tag{18}$$

with the largest eigenvalues σ_i^2.

The square roots of the eigenvalues, σ_i, are called the singular values and the eigenvectors $v_i(t_0)$ the (right) singular vectors of L with respect to the inner product E (see, e.g., Noble & Daniel, 1977). The singular vectors with largest singular values identify the directions characterized by maximum growth. The time interval $t - t_0$ is called optimization time interval.

Unlike L itself, the operator $L^{*E}L$ is normal. Hence, its eigenvectors $v_i(t_0)$ can be chosen to form a complete orthonormal basis in the Nth -dimensional tangent space of the perturbations at χ_0. Moreover, the eigenvalues are real, $\sigma_i^2 \geq 0$.

At optimization time t, the singular vectors evolve to

$$v_i(t) = L(t, t_0)v_i(t_0) \tag{19}$$

which in turn satisfy the eigenvector equation

$$LL^{*E}v_i(t) = \sigma_i^2 v_i(t_0) \tag{20}$$

From Eqs. (17) and (20) it follows that

$$\|v_i(t)\|_E^2 = \sigma_i^2 \tag{21}$$

Since any perturbation $x(t) / \|x(t_0)\|_E$ can be written as a linear combination of the singular vectors v_i, it follows that

$$\max_{\|x(t_0)\|_E}\left(\frac{\|x(t)\|_E}{\|x(t_0)\|_E}\right) = \sigma_1 \tag{22}$$

Thus, maximum growth as measured by the norm $\|\dots\|_E$ is associated with the dominant singular vector v_1.

Given the tangent forward propagator L, it is evident from Eq. (18) that singular vectors' characteristics depend strongly on the inner product definition and to the specification of the optimization time interval.

The problem can be generalized by selecting a different inner product at initial and optimization time. Consider two inner products defined by the (positive definite Hermitian) matrices E_0 and E, and re-state the problem as finding the phase space directions x for which

$$\frac{\|x(t)\|_E}{\|x(t_0)\|_E} = \frac{\langle Lx(t_0); ELx(t_0)\rangle}{\langle x(t_0); E_0 x(t_0)\rangle} \tag{23}$$

is maximum. Applying the transformation $y = E_0^{1/2}$, the right hand side of Eq. (18) can be transformed into

$$\frac{\langle LE_0^{-1/2}y(t_0); ELE_0^{-1/2}y(t_0)\rangle}{\langle y(t_0); y(t_0)\rangle} = \frac{\langle y(t_0); E_0^{-1/2}L^* ELE_0^{-1/2}y(t_0)\rangle}{\langle y(t_0); y(t_0)\rangle} \tag{24}$$

Since

$$E_0^{-1/2}L^* ELE_0^{-1/2} = (E^{-1/2}LE_0^{-1/2})^* (E^{-1/2}LE_0^{-1/2}) \tag{25}$$

the phase space directions which maximize the ratio in Eq. (24) are the singular vectors of the operator $E^{-1/2}LE_0^{-1/2}$ with respect to the canonical Euclidean inner product. With this definition, the dependence of the singular vectors' characteristics on the inner products is made explicit.

At ECMWF, due to the very large dimension of the system, the eigenvalue problem that defines the singular vectors is solved by applying a Lanczos code (Glub & Van Loan 1983).

APPENDIX B PROJECTION OPERATORS

The set of differential equations that defines the system evolution can be solved numerically with different methods. For example, they can be solved with spectral methods, by expanding a state vector onto a suitable basis of functions, or with finite-difference methods in which the derivatives in the differential equation of motions are replaced by finite difference approximations at a discrete set of grid points in space. The ECMWF primitive equation model solves the system evolution equations partly in spectral space, and partly in grid point space.

Denote by x_g the grid point representation of the state vector x, by S the spectral-to-grid point transformation operator, $x_g = Sx$, and by Gx_g the multiplication of the vector x_g, defined in grid-point space, by the function $g(s)$:

$$g(s) = 1 \forall s \in \Sigma$$
$$g(s) = 0 \forall s \notin \Sigma \tag{26}$$

where s defines the coordinate of a grid point, and Σ is a geographical region.

Define the function $w(n)$ in spectral space as

$$w(n) = 1 \forall n \in \Omega$$
$$w(n) = 0 \forall n \notin \Omega \tag{27}$$

where n identifies a wave number and Ω is a sub-space of the spectral space.

Consider a vector x. The application of the local projection operator T defined as

$$T = S^{-1}GS \tag{28}$$

to the vector x sets the vector x to zero for all grid points outside the geographical region Σ. Similarly, the application of the spectral projection operator W to the vector x sets to zero its spectral components with wave number outside Ω.

The projection operators T and W can be used either at initial or at final time, or at both times. As an example, these operators can be used to formulate the following problem: find the perturbations with (i) the fastest growth during the time interval $t - t_0$, (ii) unitary E_0-norm and wave components belonging to Ω_0 at initial time, (iii) maximum E-norm inside the geographical region Σ and wave components belonging to Ω_1 at optimization time. This problem can be solved by the computation of the singular values of the operator

$$K = E^{-1/2} T S_1 L S_0 E_0^{-1/2} \qquad (29)$$

REFERENCES

Appenzeller, Ch., Davies, H. C., Popovic, J. M., Nickovic, S., & Gavrilov, M. B., 1996: PV morphology of a frontal-wave development. Met. and Atm. Phys., 58, 21-40.

Barkmeijer, J., van Gijzen, M., & Bouttier, F., 1998: Singular vectors and estimates of the analysis error covariance metric. Q. J. R. Meteor. Soc., 124, 549, 1695-1713.

Barkmeijer, J., Buizza, R., & Palmer, T. N., 1999a: 3D-Var Hessian singular vectors and their potential use in the ECMWF Ensemble Prediction System. Q. J. R. Meteor. Soc., 125, 2333-2351.

Barkmeijer, J., Buizza, R., Palmer, T. N., & Puri, K., 1999b: Tropical singular vectors computed with linearized diabatic physics. Q. J. R. Meteor. Soc., submitted.

Bishop, C. H., & Toth, Z., 1998: Ensemble Transformation and Adaptive Observations. J. Atmos. Sci., under revision.

Borges, M., & Hartmann, D. L., 1992: Barotropic instability and optimal perturbations of observed non-zonal flows. J. Atmos. Sci., 49, 335-354.

Buizza, R., 1992: Unstable perturbations computed using the adjoint technique. ECMWF Research Department Technical Memorandum No. 189, ECMWF, Shinfield Park, Reading RG2 9AX, UK.

Buizza, R., 1994: Sensitivity of Optimal Unstable Structures. Q. J. R. Meteorol. Soc., 120, 429-451.

Buizza, R., 1997: The singular vector approach to the analysis of perturbation growth in the atmosphere. Ph. D. thesis, University College London, Gower Street, London.

Buizza, R., & Palmer, T. N., 1995: The singular-vector structure of the atmospheric general circulation. J. Atmos. Sci., 52, 9, 1434-1456.

Buizza, R., & Montani, A., 1999: Targeting observations using singular vectors. J. Atmos. Sci., 56, 2965-2985.

Buizza, R., Tribbia, J., Molteni, F., & Palmer, T. N., 1993: Computation of optimal unstable structures for a numerical weather prediction model. Tellus, 45A, 388-407.

Buizza, R., Petroliagis, T., Palmer, T. N., Barkmeijer, J., Hamrud, M., Hollingsworth, A., Simmons, A., & Wedi, N., 1998: Impact of model resolution and ensemble size on the performance of an ensemble prediction system. Q. J. R. Meteorol. Soc., 124, 1935-1960.

Buizza, R., Miller, M., & Palmer, T. N., 1999: Stochastic simulation of model uncertainties. Q. J. R. Meteorol. Soc., 125, 2887-2908.

Charney, J. G., 1947: The dynamics of long waves in a baroclinic westerly current. J. Meteor., 4, 135-162.

Charney, J. G., 1948: On the scale of atmospheric motions. Geofys. Publ., 17, 1-17.

Courtier, P., Freydier, C., Geleyn, J.-F., Rabier, F., & Rochas, M., 1991: The Arpege project at Météo-France. Proceedings of the ECMWF Seminar on Numerical methods in atmospheric models, Vol. II, 193-231. ECMWF, Shinfield Park, Reading RG2 9AX, UK.

Courtier, P., Derber, J., Errico, R., Louis, J.-F., & Vukicevic, T., 1993: Important literature on the use of adjoint, variational methods and the Kalman filter in meteorology. Tellus, 45A, 342-357.

Courtier, P., Thepaut, J.-N., & Hollingsworth, A., 1994: A strategy for operational implementation of 4D-Var, using an incremental approach. Q. J. R. Meteorol. Soc., 120, 1367-1388.

Downton, R. A., & Bell, R. S., 1988: The impact of analysis differences on a medium-range forecast. Meteorol. Mag., 117, 279-285.

Ehrendorfer, M., 1994: The Liouville equation and its potential usefulness for the prediction of forecast skill. Part I: Theory. Mon. Wea. Rev., 122, 703-713.

Ehrendorfer, M., & Tribbia, J. J., 1995: Efficient prediction of covariances using singular vectors. Preprint Volume, 6th International Meeting on Statistical Climatology, Galway, Ireland, 135-138.

Epstein, E. S., 1969: Stochastic dynamic prediction. Tellus, 21, 739-759.

Evensen, G., 1994: Sequential data assimilation with a non-linear quasi-geostrophic model using Monte Carlo methods to forecast error statistics. J. Geoph. Res., 99, 10,143-10,162.

Farrell, B. F., 1982: The initial growth of disturbances in a baroclinic flow. J. Atmos. Sci., 39, 8, 1663-1686.

Farrell, B. F., 1988: Optimal excitation of neutral Rossby waves. J. Atmos. Sci., 45 (2), 163-172.

Farrell, B. F., 1989: Optimal excitation of baroclinic waves. J. Atmos. Sci., 46 (9), 1193-1206.

Fleming, R. J., 1971a: On stochastic dynamic prediction. I: the energetics of uncertainty and the question of closure. Mon. Wea. Rev., 99, 851-872.

Fleming, R. J., 1971b: On stochastic dynamic prediction. II: predictability and utility. Mon. Wea. Rev., 99, 927-938.

Gleeson, T. A., 1970: Statistical-dynamical predictions. J. Appl. Meteorol., 9, 333-344.

Golub, G. H., & Van Loan, C. F., 1983: Matrix computation. North Oxford Academic Publ. Co. Ltd., pp. 476.

Hall, M. C. G., & Cacuci, D. G., 1983: Physical interpretation of the adjoint functions for sensitivity analysis of atmospheric models. J. Atmos. Sci., 46, 9, 1193-1206.

Holton, J. R., 1992: An Introduction to Dynamic Meteorology. Academic Press Inc., 511 pp.

Holland, G. J., McGeer, T., & Youngren, H., 1992: Autonomous aerosondes for economical atmospheric soundings anywhere on the globe. Bull. Amer. Met. Soc., 73, 1987-1998.

Hoskins, B. J., & Valdes, P. J., 1990: On the exhistence of storm tracks. J. Atmos. Sci., 47, 1854-1864.

Hoskins, B. J., McIntyre, M. E., & Robertson, A. W., 1985: On the use and significance of isentropic potential vorticity maps. Q. J. R. Meteorol. Soc., 111, 877-946.

Hoskins, B. J., Buizza, R., & Badger, J., 1999: The nature of singular vector growth and structure. Q. J. R. Meteorol. Soc., under revision.

Harrison, M. S. J., Palmer, T. N., Richardson, D. S., & Buizza, R., : 1999: Analysis and model dependencies in medium-range ensembles: two transplant case studies. Q. J. R. Meteorol. Soc., 125, 2487-2515.

Houtekamer, P. L., Lefaivre, L., Derome, J., Ritchie, H., & Mitchell, H., 1996: A system simulation approach to ensemble prediction. Mon. Wea. Rev., 124, 1225-1242.

Houtekamer, P. L., & Mitchell, H., 1998: Data assimilation using an ensemble Kalman filter. Mon. Wea. Rev., 126, 796-811.

Jacob, C., 1994: The impact of the new cloud scheme on ECMWF's Integrated Forecasting System (IFS). Proceedings of the ECMWF/GEWEX workshop on Modeling, validation and assimilation of clouds, ECMWF, Shinfield Park, Reading RG2 9AX, 31 October - 4 November 1994, pp. 464.

Joly, A., Jorgensen, D., Shapiro, M. A., Thorpe, A. J., Bessemoulin, P., Browning, K. A., Cammas, J.-P., Chalon, J.-P., Clough, S. A., Emanuel, K. A., Eymard, R., Gall, R., Hildebrand, P. H., Langland, R. H., Lamaître, Y., Lynch, P., Moore, J. A., Persson, P. O. G., Snyder, C., & Wakimoto, R. M., 1996: The Fronts and Atlantic Storm-Track Experiment (FASTEX): Scientific objectives and experimental design. Report Number 6. The FASTEX Project Office, Météo-France, CNRM, 42 Avenue Coriolis, Toulouse, France. (Also submitted to Bull. Am. Met. Soc.).

Kontarev, G., 1980: The adjoint equation technique applied to meteorological problems. Technical Report No. 21, European Centre for Medium-Range Weather Forecasts, Shinfield Park, Reading RG2 9AX, UK.

Lacarra, J.-F., & Talagrand, O., 1988: Short range evolution of small perturbations in a barotropic model. Tellus, 40A, 81-95.

Langland, R H, & Rohaly, G D, 1996: Adjoint-based targeting of observations for FASTEX cyclones. American Meteorological Society pre-prints of the 7th conference on mesoscale processes, September 9-13, 1996, Reading, UK, pp. 618.

Le Dimet, F.-X., & Talagrand, O., 1986: Variational algorithms for analysis and assimilation of meteorological observations: theoretical aspects. Tellus, 38A, 97-110.

Leith, C. E., 1974: Theoretical skill of Monte Carlo forecasts. Mon. Wea. Rev., 102, 409-418.

Lorenz, E. N., 1963: Deterministic non-periodic flow. J. Atmos. Sci., 20, 130-141.

Lorenz, E. N., 1965: A study of the predictability of a 28-variable atmospheric model. Tellus, 17, 321-333.

Lorenz, E. N., 1993: The essence of chaos. UCL Press, pp 227.

Mahfouf, J.-F., 1999: Influence of physical processes on the tangent-linear approximation. Tellus, 51A, 147-166.

Marsigli, C., Montani, A., Nerozzi, F., Paccagnella, T., Molteni, F., & Buizza, R., 1999b: High resolution ensemble prediction. Part II: an application to four flood events. Q. J. R. Meteorol. Soc., submitted

Morcrette, J.-J., 1990: Impact of changes to the radiation transfer parameterisation plus cloud optical properties in the ECMWF model. Mon. Wea. Rev., 118, 847-873.

Molteni, F., & Palmer, T. N., 1993: Predictability and finite-time instability of the northern winter circulation. Q. J. R. Meteorol. Soc., 119, 1088-1097.

Molteni, F., Buizza, R., Palmer, T. N., & Petroliagis, T., 1996: The new ECMWF ensemble prediction system: methodology and validation. Q. J. R. Meteorol. Soc., 122, 73-119.

Molteni, F., Buizza, R., Marsigli, C., Montani, A., Nerozzi, F., & Paccagnella, T., 1999: High resolution ensemble prediction. Part I: representative members definition and global applications. Q. J. R. Meteorol. Soc., submitted.

Montani, A., Thorpe, A. J., Buizza, R., & Unden, P., 1999: Forecast skill in the ECMWF model using targeted ob-

servations during FASTEX. Q. J. R. Meteorol. Soc., in press.

Noble, B., & Daniel, J. W., 1977: Applied linear algebra, Prenctice-Hall, Inc., pp. 477.

Palmer, T. N., 1997: On parametrizing scales that are only somewhat smaller than the smallest resolved scales, with application to convection and orography. Proceedings of the ECMWF workshop on New insights and approaches to convective parametrization, ECMWF, Shinfield Park, Reading RG2-9AX, UK, 328-337.

Palmer, T. N., Molteni, F., Mureau, R., Buizza, R., Chapelet, P., & Tribbia, J., 1993: Ensemble prediction. Proceedings of the ECMWF Seminar on Validation of models over Europe: vol. I, ECMWF, Shinfield Park, Reading, RG2 9AX, UK.

Pu, Z.-X., Kalnay, E., Sela, J., & Szunyogh., 1997: Sensitivity of forecast error to initial conditions with a quasi-inverse linear method. Mon. Wea. Rev., 125, 2479-2503.

Pu, Z.-X., Kalnay, E., & Toth, Z., 1998: Application of the quasi-inverse linear and adjoint NCEP global models to targeted observations during FASTEX. Pre-prints of the 12th Conference on Numerical Weather Prediction, 11-16 January 1998, Phoenix, Arizona, 8-9.

Puri, K., Barkmeijer, J., & Palmer, T. N., 1999: Ensemble prediction of tropical cyclones using targeted diabatic singular vectors. Q. J. R. Meteorol. Soc., submitted.

Rabier, F., Klinker, E., Courtier, P., & Hollingsworth, A, 1996: Sensitivity of forecast errors to initial conditions. Q. J. R. Meteorol. Soc., 122, 121-150.

Richardson, L. F., 1922: Weather Prediction by Numerical Process. Cambridge University Press (reprt. Dover, New York).

Richardson, D. S., 1998: The relative effect of model and analysis differences on ECMWF and UKMO operational forecasts. Proceedings of the ECMWF Workshop on Predictability, ECMWF, Shinfield Park, Reading RG2 9AX, UK.

Simmons, A. J., Burridge, D. M., Jarraud, M., Girard, C., & Wergen, W., 1989: The ECMWF medium-range prediction models development of the numerical formulations and the impact of increased resolution. Meteorol. Atmos. Phys., 40, 28-60.

Simmons, A. J., Mureau, R., & Petroliagis, T., 1995: Error growth and predictability estimates for the ECMWF forecasting system. Q. J. R. Meteorol. Soc., 121, 1739-1771.

Snyder, C., 1996: Summary of an informal workshop on adaptive observations and FASTEX. Bull. Am. Meteor. Soc., 77, 953-961.

Somerville, R. C. J., 1979: Predictability and prediction of ultra-long planetary waves. Pre-prints of the Amer. Meteor. Soc. Fourth Conference on Numerical Weather Prediction, Silver Spring, MD, 182-185.

Strang, G., 1986: Introduction to applied mathematics. Wellesley-Cambridge Press, pp 758.

Thorpe, A. J., & Shapiro, M. A., 1995: FASTEX: Fronts and Atlantic Storm Track Experiment. The Science Plan. Available form the FASTEX Project Office, July 1995, pp. 25.

Thorpe, A. J., Buizza, R., Montani, A., & Palmer, T. N., 1998: Chaotic control for weather prediction. Royal Society New frontiers in Science Exhibition, June 1998, The Royal Society, 6 Carlton House Terrace, London SW1Y-5AG, UK.

Tiedtke, M., 1993: Representation of clouds in large-scale models. Mon. Wea. Rev., 121, 3040-3060.

Toth, Z., & Kalnay, E., 1993: Ensemble forecasting at NMC: the generation of perturbations. Bull. Am. Met. Soc.,

74, 2317-2330.

Tracton, M. S., & Kalnay, E., 1993: Operational ensemble prediction at the National Meteorological Center: practical aspects. Weather and Forecasting, 8, 379-398.

Urban, B., 1985: Error maximum growth in simple meteorological models (in French). Meteorologie Nationale Internal Report.

Viterbo, P., & Beljaars, C. M., 1995: An improved land surface parametrisation scheme in the ECMWF model and its validation. J. Clim., 8, 2716-2748.

Von Neumann, J., & Richtmeyer, R. D., 1950: A method for the numerical calculation of hydrodynamical shocks. J. Appl. Phys., 21, 232.